Error modeling of multi-baseline optical truss, part II: application to SIM metrology truss field dependent error

L. D. Zhang[a,b], Mark Milman[a], Robert Korechoff[a]
[a]Jet Propulsion Laboratory, 4800 Oak Grove Dr, Pasadena, CA 91109
[b]Columbus Technologies & Services, 225 S. Lake Ave, Ste 1010, Pasadena, CA 91101

ABSTRACT

The current design of the Space Interferometry Mission (SIM) employs a 19 laser-metrology-beam system (also called L19 external metrology truss) to monitor changes of distances between the fiducials of the flight system's multiple baselines. The function of the external metrology truss is to aid in the determination of the time-variations of the interferometer baseline. The largest contributor to truss error occurs in SIM wide-angle observations when the articulation of the siderostat mirrors (in order to gather starlight from different sky coordinates) brings to light systematic errors due to offsets at levels of instrument components (which include corner cube retro-reflectors, etc.). This error is labeled external metrology wide-angle field-dependent error. Physics-based model of field-dependent error at single metrology gauge level is developed and linearly propagated to errors in interferometer delay. In this manner delay error sensitivity to various error parameters or their combination can be studied using eigenvalue/eigenvector analysis. Also validation of physics-based field-dependent model on SIM testbed lends support to the present approach. As a first example, dihedral error model is developed for the corner cubes (CC) attached to the siderostat mirrors. Then the delay errors due to this effect can be characterized using the eigenvectors of composite CC dihedral error. The essence of the linear error model is contained in an error-mapping matrix. A corresponding Zernike component matrix approach is developed in parallel, first for convenience of describing the RMS of errors across the field-of-regard (FOR), and second for convenience of combining with additional models. Average and worst case residual errors are computed when various orders of field-dependent terms are removed from the delay error. Results of the residual errors are important in arriving at external metrology system component requirements. Double CCs with ideally co-incident vertices reside with the siderostat. The non-common vertex error (NCVE) is treated as a second example. Finally combination of models, and various other errors are discussed.

Keywords: modeling, interferometer, metrology, corner cube retro-reflector, instrument systematic error

1. INTRODUCTION

Space Interferometry Mission (SIM) is a space optical interferometer mission designed to achieve unprecedented accuracy of stellar astrometry[1]. Since most of the astrometric target stars are very dim, substantial integration time is required for measuring starlight fringes. The SIM baseline is essentially time varying on this time scale. Variations of the baseline can be due to spacecraft attitude changes, baseline fiducial changes (systematic variations, thermal drifts, etc.), or other higher order effects. In order to track the changes of the baseline, SIM employs two guide interferometers (see Fig. 1) that observe bright "guide" stars, and a laser metrology truss system that calibrates distances between fiducials of the primary & secondary science baseline and the guide baseline. In this manner, the guide interferometers track the spacecraft attitude changes, while the metrology truss is designed to remove the systematic and temporal variations of the baseline fiducials to the best of its capacity. An overview of the SIM mission and descriptions of major instrument subsystems can be found in Refs. 2-3. Background of on-board real-time reconstruction of the baseline vector can be found in Ref. 4.

There are two observational modes in which SIM operates. They are the narrow-angle (1^0 diameter) and wide-angle (15^0 diameter) circular field of regard (FOR, also called tiles in SIM terminology) observations. Systematic Errors of the wide-angle FOR observations are much more severe than that of the narrow-angle case. We will be concerned with the wide-angle error performance modeling of the external metrology system in this paper. The external metrology system consists of 15 essential close-loop laser beams that monitor the distances between fiducials. The geometry of the current

SIM external metrology system resembles a truss (see Fig. 1 for an illustration of the SIM flight system architecture). Criticality of the links between the guide baseline and the science baseline has prompted for addition of backup laser gauges on those links, increasing the number of beams to 19. Hence the error modeling in this work is based on this so-called L19 metrology truss. Error performance of the entire SIM interferometer is outside the scope of this paper but a global error budget summary can be found in Ref. 5.

The focus of this work is on time-independent systematic errors due to field-dependent effects. The approach is to start from the physics-based model of the individual instrument component errors and develop single gauge level field-dependent error model. Then the single gauge errors are mapped to errors in the determination of baseline, which in turn propagate to errors in delay measurement. The fact that physics-based linear model of field-dependent error has been validated on SIM external metrology testbed KITE[6] lends support to this approach.

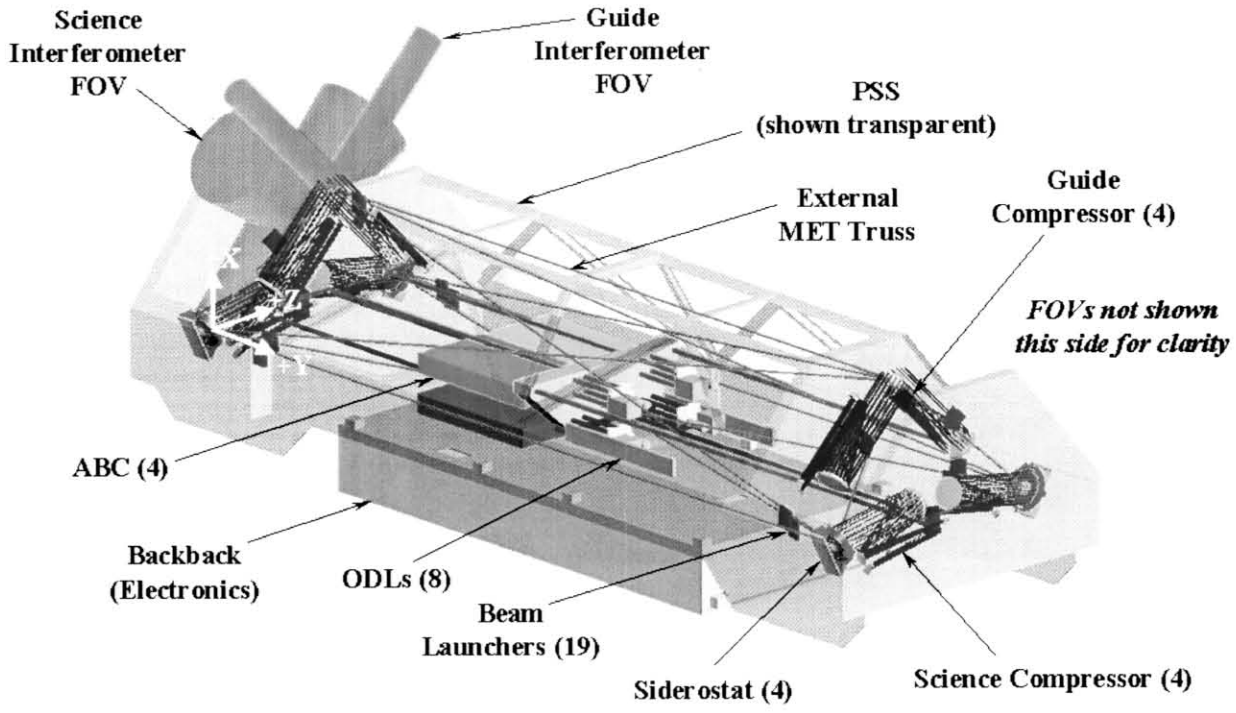

Figure 1: Illustration of the SIM flight system architecture. The global coordinate frame used for modeling is shown as the set of white X, Y, Z arrows.

In part I of this paper[5], the mathematical formulation of mappings from single gauge errors to delay error is derived. Part II of this paper develops physics-based model of single metrology gauge's field-dependent error. In section 2 the external metrology's geometry and coordinate frame are discussed. The results from part I of this paper as applied here are summarized. The details of error parameter model development are described by following through the example of dihedral error model in section 3. The non-common vertex offset error (NCVE) of the double corner cubes (CC) is treated in the following section. Finally in section 5, details of combination of models are laid out. Also various other effects are discussed.

2. L19-TRUSS FIELD-DEPENDENT ERROR

2.1 L19 truss geometry and relation to sky coordinates

The baseline fiducials/nodes appear in the L19 geometry as shown in Figure 2.

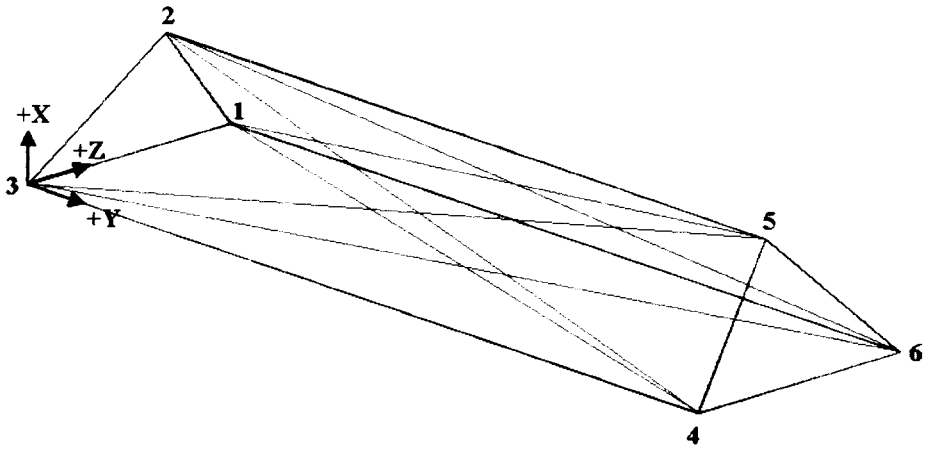

Figure 2. 3D view of the L19 truss in the global coordinate frame of the spacecraft. Primary science baseline is between fiducials 3 & 4. The secondary science baseline is 6-1. The guide baseline is 2-5.

Figure 3 illustrates the definition of sky coordinates (u, v) and its relationship to the spacecraft coordinates. The modeling in this work is done on the science baseline 6-1, which is equivalent to modeling based on baseline 3-4 if correct symmetry rules are applied.

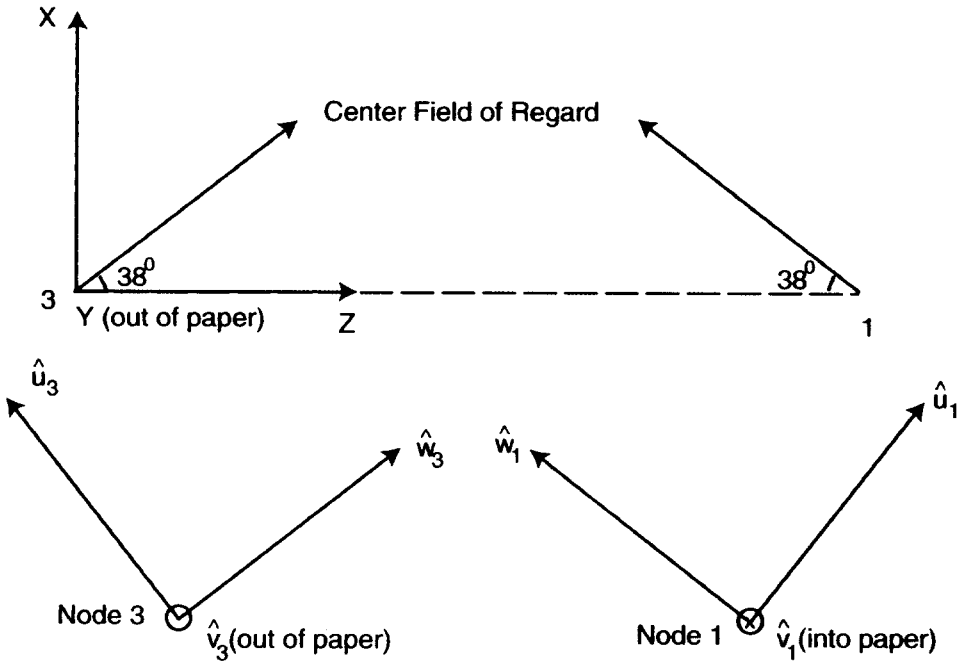

Figure 3. View of node 3 and 1 with their respective sky coordinates in the negative Y direction. The symmetry of center FOR direction between 1 and 3 is noted. For baseline $\mathbf{b}_{s1}$, the sky coordinates is (u3, v3), and the same for $\mathbf{b}_{s2}$ is (u1, v1). The coordinates of center FOR star vector $\mathbf{s}$ in the right-handed $\mathbf{u}-\mathbf{v}-\mathbf{w}$ system are conveniently written as (0, 0, 1).

If we do modeling on baseline 6-1, the starlight vector $\mathbf{s}$ will also need to be expressed in the same coordinates. The following expression will be the convention of $\mathbf{s}$ in computing the delay error from baseline 6-1:

$$\mathbf{s}(u,v) = u\,\mathbf{e}_u + v\,\mathbf{e}_v + \sqrt{1-u^2-v^2}\,\mathbf{e}_w \qquad (1)$$

$$\mathbf{e}_u = \cos(38^0)\,\mathbf{e}_x + \sin(38^0)\,\mathbf{e}_z\,, \quad \mathbf{e}_v = -\,\mathbf{e}_y\,, \quad \mathbf{e}_w = \sin(38^0)\,\mathbf{e}_x - \cos(38^0)\,\mathbf{e}_z$$

2.2 Summary of mapping from single gauge error to delay error

We first summarize the main ingredients of the single gauge model and then scope of mapping from single gauge to delay:

2.2.1 Single Gauge Model

We consider the change due to articulation in the structure. Therefore only the beams incident on the articulating CC's need to be modeled. There are altogether 8 beams on the 2 double CC's (4 CC's) located at the science baseline fiducials. The gauge model is expressed in sky coordinates (u,v).

2.2.2 From Gauge Error to Science Delay Error

In reality, there are altogether 14 laser beams operating in the external metrology system (15 if all beams were present between the 6 fiducials, but the beam between the primary science baseline fiducials is substituted with internal metrology beam instead). In keeping with the larger scheme of metrology or star calibration of fiducial positions, all the single gauge errors need to be combined in the full 14-beam gauge error vector δl, which then will be mapped to science delay error δd through the L-19 $\mathbf{M}$ matrix:

$$\delta d(u,v) = <\mathbf{s}, \delta\mathbf{b}> = <\mathbf{s}, \mathbf{M}\delta l(u,v)> \qquad (2)$$

Above $\delta\mathbf{b}$ is the error in external metrology measured baseline, δl is the combined single gauge error vector, $\mathbf{s}$ is the unit vector in the starlight direction, the notation $<\,,>$ stands for vector inner product. The reader is referred to part I of this paper[7] for derivation of equation (2).

2.2.3 Mapping Matrix

Let us define

$$\delta l = [\delta l_{12} \quad \delta l_{13} \quad \delta l_{14} \quad \delta l_{15} \quad \delta l_{23} \quad \delta l_{24} \quad \delta l_{25} \quad \delta l_{26} \quad \delta l_{34} \quad \delta l_{35} \quad \delta l_{36} \quad \delta l_{45} \quad \delta l_{46} \quad \delta l_{56}]^T \qquad (3)$$

By adapting the mapping matrix to the L19 geometry, we have:

$$\mathbf{M} = \left[\mathbf{Z}_s + \mathbf{B} * pinv(\mathbf{T}) * \mathbf{S} * \mathbf{Z}_g\right] * pinv\left[\mathbf{F}'(\mathbf{X} = \mathbf{X}^0)\right] \quad (4)$$

$$\mathbf{Z}_s = \left[\mathbf{I}_{3\times3} \quad \mathbf{0}_{3\times12} \quad -\mathbf{I}_{3\times3}\right]$$

$$\mathbf{Z}_g = \left[\mathbf{0}_{3\times3} \quad -\mathbf{I}_{3\times3} \quad \mathbf{0}_{3\times6} \quad \mathbf{I}_{3\times3} \quad \mathbf{0}_{3\times3}\right]$$

$\mathbf{I}_{s\times s}$ - identity matrix of order s

$\mathbf{0}_{s\times t}$ - zero matrix of size s×t

$\mathbf{X} = \left[\mathbf{X}_1^T \quad \mathbf{X}_2^T \quad \mathbf{X}_3^T \quad \mathbf{X}_4^T \quad \mathbf{X}_5^T \quad \mathbf{X}_6^T\right]^T$ is a 18×1 vector

$\mathbf{X}_i$ - 3×1 position vector of fiducial i

$\mathbf{X}_i^0$ - known position of fiducial i

$\mathbf{F}'(\mathbf{X}) = \dfrac{1}{\delta \mathbf{X}^T} * \delta l$, 14×18 matrix

δl - defined in equation (14), $\delta l_{ij} = \left|\mathbf{X}_j - \mathbf{X}_i\right| - \left|\mathbf{X}_j^0 - \mathbf{X}_i^0\right|$.

pinv() - pseudo-inverse of matrix

$$\mathbf{S} = \begin{bmatrix} s_{g1}^T \\ s_{g2}^T \end{bmatrix}, \quad \mathbf{T} = \begin{bmatrix} \left(b_g \times s_{g1}\right)^T \\ \left(b_g \times s_{g2}\right)^T \end{bmatrix}$$

$s_{g1,2}$ are the 2 guide star vectors of size 3×1, $b_g = \mathbf{X}_5^0 - \mathbf{X}_2^0$ is also 3×1 vector

B is the skew symmetric matrix, such that for vector x, $\mathbf{B}x = b_s \times x$.

$b_s = \mathbf{X}_1^0 - \mathbf{X}_6^0$ is the science baseline

3. DIHEDRAL ERROR MODEL

3.1 Basic parameters

For each CC, three facet unit normal vectoes are labeled as $\mathbf{n}_1, \mathbf{n}_2, \mathbf{n}_3$. The three components of the dihedral error are defined as:

$$\mathbf{a} = \left[a_1 \quad a_2 \quad a_3\right]^T, \quad d\mathbf{n}_2 = a_3\mathbf{n}_1, \quad d\mathbf{n}_3 = -a_2\mathbf{n}_1 + a_1\mathbf{n}_2 \quad (5).$$

3.2 From CC dihedral error to delay error

We derive a general scheme of mapping from dihedral errors on the 4 articulating CC's to the delay error. Of all the gauge measurements listed in equation (3), only a subset composed of $\delta l_{12}, \delta l_{13}, \delta l_{14}, \delta l_{15}$ and $\delta l_{26}, \delta l_{36}, \delta l_{46}, \delta l_{56}$ will change during siderostat articulation. So we compose a subset gauge measurement vector

$$\delta l_s = \left[\delta l_{12} \quad \delta l_{13} \quad \delta l_{14} \quad \delta l_{15} \quad \delta l_{26} \quad \delta l_{36} \quad \delta l_{46} \quad \delta l_{56}\right]^T \quad (6)$$

which satisfies

$$\delta l = Z_E \cdot \delta l_s$$

$$Z_E = \begin{bmatrix} 1 & 0 & & & & & & \\ 0 & 1 & & & & & & \\ & & 1 & 0 & & & & \\ & & 0 & 1 & & & & \\ & & 0 & 0 & & & & \\ & & 0 & 0 & & & & \\ & & 0 & 0 & & & & \\ & & & & 1 & 0 & & \\ & & & & 0 & 0 & & \\ & & & & 0 & 0 & & \\ & & & & 0 & 1 & & \\ & & & & 0 & 0 & & \\ & & & & & & 1 & 0 \\ & & & & & & 0 & 1 \end{bmatrix} \tag{7}$$

Call it external metrology design matrix if you will, Z_E defined in equation (7), is a 14×8 matrix with only non-zero elements at the specified locations. Let us also define the dihedral errors of the 4 articulating CC's as a single parameter vector of size 12×1:

$$\mathbf{a} = \left[\left(\mathbf{a}^1\right)^T \quad \left(\mathbf{a}^2\right)^T \quad \left(\mathbf{a}^3\right)^T \quad \left(\mathbf{a}^4\right)^T \right]^T, \quad \mathbf{a}^i = \left[a_1^i \quad a_2^i \quad a_3^i \right]^T, \; i = 1,2,3 \tag{8}$$

In the above equation $\mathbf{a}^i$, $i = 1, 2, 3, 4$ are the 4 articulating CC's (In the L19 designation of Table A1, the order of CCs from $i = 1$ to $i = 4$ is 1.a, 1.c; 6.c, 6.a. Please note that CC 6.c is the mirror image of CC 1.c about the XZ plane that exactly halves the truss structure, *i.e.*, the surface normals are exactly opposite in y components. The reader is encouraged to verify this using Table A1 and the illustration in Figure 1.) dihedral error vectors (of size 3×1, defined in equation (5)). Because the gauge errors are linear with respect to dihedral error parameters, δl_s can be written as:

$$\delta l_s(u,v) = \frac{dl_s}{d\mathbf{a}^T} \cdot \mathbf{a}$$

$$= \frac{1}{\sigma_a} \begin{bmatrix} (d\mathbf{l}_{12})^T & 0_{1\times3} & 0_{1\times3} & 0_{1\times3} \\ (d\mathbf{l}_{13})^T & 0_{1\times3} & 0_{1\times3} & 0_{1\times3} \\ 0_{1\times3} & (d\mathbf{l}_{14})^T & 0_{1\times3} & 0_{1\times3} \\ 0_{1\times3} & (d\mathbf{l}_{15})^T & 0_{1\times3} & 0_{1\times3} \\ 0_{1\times3} & 0_{1\times3} & (d\mathbf{l}_{26})^T & 0_{1\times3} \\ 0_{1\times3} & 0_{1\times3} & (d\mathbf{l}_{36})^T & 0_{1\times3} \\ 0_{1\times3} & 0_{1\times3} & 0_{1\times3} & (d\mathbf{l}_{46})^T \\ 0_{1\times3} & 0_{1\times3} & 0_{1\times3} & (d\mathbf{l}_{56})^T \end{bmatrix} \begin{bmatrix} \mathbf{a}^1 \\ \mathbf{a}^2 \\ \mathbf{a}^3 \\ \mathbf{a}^4 \end{bmatrix} \qquad (8)$$

In general we use the notation $0_{m\times n}$ for a $m\times n$ matrix of zeros. The $d\mathbf{l}_{ij}(u,v)$ are the single gauge models. They have been computed using fundamental vector geometry of rays reflecting of corner cubes[8]. Now the delay error due to dihedrals can be written as:

$$\delta d = \left\langle \mathbf{s}, \mathbf{M} Z_E \frac{dl_s}{d\mathbf{a}^T} \mathbf{a} \right\rangle \qquad (9)$$

Defining a new field-dependent matrix

$$\mathbf{g}(u,v) = \left[\mathbf{s}(u,v)\right]^T \mathbf{M} Z_E \frac{dl_s(u,v)}{d\mathbf{a}^T} \qquad (10)$$

of size 1×12, we can rewrite the delay error

$$\delta d(u,v) = \mathbf{g}(u,v)\,\mathbf{a} \qquad (11)$$

4. NON-COMMON VERTEX ERROR MODEL

4.1 Introduction to NCVE

Figure 2 illustrates the basic parameters associated with a double corner cube at one of the siderostat mirrors. Let 1.a and 1.c designate the 2 CCs residing at the "same" vertex.

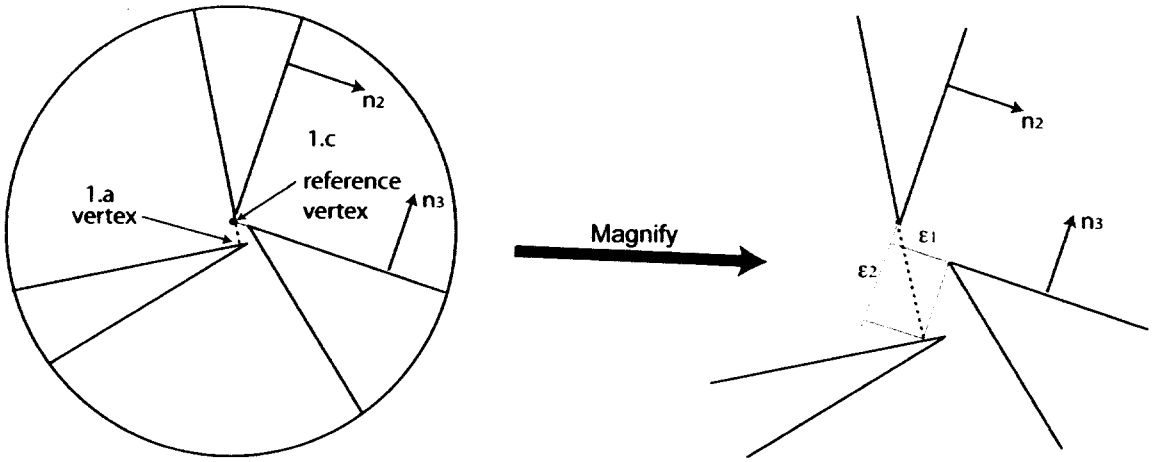

Figure 2: Illustration at fiducial #1 of the geometry associated with the definition of error parameters. The view is top-down along the normal direction of the shared surface of the double corner cube. The reference corner cube is labeled as 1.c in the L19 designation. Corner cubes are formed by the presence of the wedges. And the vertex is effectively the intersect of non-connect surfaces. The central portion is drawn in magnified details on the right.

4.2 Parameters and the model

Let vector Δ_1 denote the offset of corner cube 1.a's vertex from that of 1.c. Since corner cube 1.a and 1.c share a common surface (the shared unit normal vector of which is labeled $\mathbf{n}_1$), the current strategy of NCVE model is only considering the offset Δ_1 to lie in the common surface (which corresponds to the reality of the manufacturing process). At center field of regard (that is $u = v = 0$), the offset is

$$\Delta_1(0,0) = \varepsilon_1 \mathbf{n}_2 + \varepsilon_2 \mathbf{n}_3 \qquad (12)$$

where $\mathbf{n}_2$ and $\mathbf{n}_3$ are the unit normals of the other 2 surfaces of 1.c. The articulation of the corner cube is taken to be performed at the vertex of 1.c. We will consider the case when there is no offset of the SIM gimbal axes from the vertex of 1.c (Consideration when there is an offset shows that the field dependent error to be the same[1].). The field dependent error results from the vertex offset vector's change due to articulation, which can be expressed as

$$\Delta_1(u,v) = \mathbb{R}(u,v)\Delta_1(0,0) \qquad (13)$$

where the rotation matrix $\mathbb{R}(u,v)$ for SIM truss articulation is derived in appendix I of Ref. 8.

The field dependent gauges that are affected by NCVE are $l_{12}, l_{13}, l_{46}, l_{56}$. Consider for example the gauge between the fiducial 1 and 2, to first order in offset, the gauge error is the projection of the Δ_1 vector onto the unit vector that

---

[1] First the reader should understand that the offset of gimbal axes from the reference CC's vertex is not an error of the truss, because the external metrology system will properly track the motion of the reference CC's vertex which is the fiducial of the science baseline. However, when there is an offset of the gimbal axes, the amount of vertex offset after articulation is different from the case when there is no offset of the gimbal axes. Without loss of generality, let us assume that the 2 gimbal axes lie in the same plane, and the intersection of the 2 axes has a vector offset Δ_g from the reference vertex of 1.c. The field dependent vertex offset is then

$$\Delta_1(u,v) = \mathbb{R}(u,v)\left(\Delta_1(0,0) - \Delta_g\right) + \mathbb{R}(u,v)\Delta_g = \mathbb{R}(u,v)\Delta_1(0,0)$$

which is the same as that of equation (2) for the case when there is no gimbal axes offset.

connects the fiducial from 2 to 1. The reason for this becomes apparent from considering the geometry as illustrated Figure 2. The gauge error is simply the difference of the measured distance $l_{1'2}$ and the designed distance l_{12}:

$$\delta l_{12} = l_{1'2} - l_{12} \qquad (14)$$

Let the unit vector pointing from fiducial 2 to 1 be $\mathbf{v}_{21}$. The vertex offset vector $\boldsymbol{\Delta}_1$ has components parallel and perpendicular to $\mathbf{v}_{21}$. For small offset, the parallel component is first order in error and the perpendicular component is second order in error.

Hence, the field-dependent error associated with the gauge between fiducial 1 and 2 is

$$\delta l_{12}(u,v) = \boldsymbol{\Delta}_1(u,v)\cdot\mathbf{v}_{21} \qquad (15a)$$

In the same manner,

$$\delta l_{13}(u,v) = \boldsymbol{\Delta}_1(u,v)\cdot\mathbf{v}_{31} \qquad (15b)$$

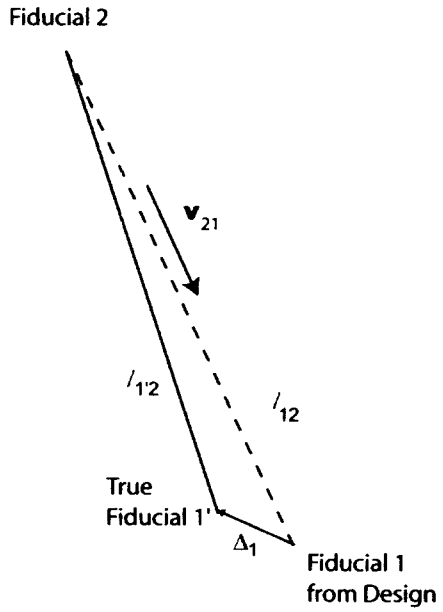

Figure 3: Illustration of the single gauge error due to an offset of the CC vertex. See text for detailed explanation.

Let the offset vector at fiducial 6 be

$$\boldsymbol{\Delta}_6(0,0) = \varepsilon_3\mathbf{n}_2' + \varepsilon_4\mathbf{n}_3' \qquad (16)$$

where the normals $\mathbf{n}_2'$ and $\mathbf{n}_3'$ are the mirror image of $\mathbf{n}_2$ and $\mathbf{n}_3$ respectively about the XZ plane in the L19 global coordinate frame. Specifically

$$\mathbf{n}_2' = \mathbf{n}_2 - 2(\mathbf{n}_2\cdot\mathbf{e}_y)\mathbf{e}_y \qquad (17)$$

$$\mathbf{n}_3' = \mathbf{n}_3 - 2(\mathbf{n}_3\cdot\mathbf{e}_y)\mathbf{e}_y$$

Gauge errors at fiducial 6 are

$$\delta l_{46}(u,v) = \boldsymbol{\Delta}_6(u,v)\cdot\mathbf{v}_{46} \qquad (18)$$

$$\delta l_{56}(u,v) = \boldsymbol{\Delta}_6(u,v)\cdot\mathbf{v}_{56}$$

where the field dependent vertex offset $\boldsymbol{\Delta}_6(u,v)$ is calculated in the same way as in equation (13), and the unit vectors $\mathbf{v}_{46}$ and $\mathbf{v}_{56}$ are the mirror images of the $\mathbf{v}_{31}$ and $\mathbf{v}_{21}$ respectively in the global Y coordinate direction:

$$\mathbf{v}_{46} = \mathbf{v}_{31} - 2\left(\mathbf{v}_{31}\cdot\mathbf{e}_y\right)\mathbf{e}_y \qquad (19)$$

$$\mathbf{v}_{56} = \mathbf{v}_{21} - 2\left(\mathbf{v}_{21}\cdot\mathbf{e}_y\right)\mathbf{e}_y$$

Rewriting the single gauge errors in the matrix form, we have

$$\begin{bmatrix}\delta l_{12}(u,v)\\ \delta l_{13}(u,v)\\ \delta l_{46}(u,v)\\ \delta l_{56}(u,v)\end{bmatrix} = \begin{bmatrix}\Delta_1(u,v)\cdot\mathbf{v}_{21}\\ \Delta_1(u,v)\cdot\mathbf{v}_{31}\\ \Delta_6(u,v)\cdot\mathbf{v}_{46}\\ \Delta_6(u,v)\cdot\mathbf{v}_{56}\end{bmatrix} = \begin{bmatrix}\left[\mathbb{R}(u,v)\left(\varepsilon_1\mathbf{n}_2+\varepsilon_2\mathbf{n}_3\right)\right]\cdot\mathbf{v}_{21}\\ \left[\mathbb{R}(u,v)\left(\varepsilon_1\mathbf{n}_2+\varepsilon_2\mathbf{n}_3\right)\right]\cdot\mathbf{v}_{31}\\ \left[\mathbb{R}(u,v)\left(\varepsilon_3\mathbf{n}_2'+\varepsilon_4\mathbf{n}_3'\right)\right]\cdot\mathbf{v}_{46}\\ \left[\mathbb{R}(u,v)\left(\varepsilon_3\mathbf{n}_2'+\varepsilon_4\mathbf{n}_3'\right)\right]\cdot\mathbf{v}_{56}\end{bmatrix} = \frac{d\mathbf{L}}{d\boldsymbol{\varepsilon}^T}\cdot\boldsymbol{\varepsilon} \qquad (20)$$

$$\frac{d\mathbf{L}(u,v)}{d\boldsymbol{\varepsilon}^T} = \begin{bmatrix}\mathbb{R}\mathbf{n}_2\cdot\mathbf{v}_{21} & \mathbb{R}\mathbf{n}_3\cdot\mathbf{v}_{21} & 0 & 0\\ \mathbb{R}\mathbf{n}_2\cdot\mathbf{v}_{31} & \mathbb{R}\mathbf{n}_3\cdot\mathbf{v}_{31} & 0 & 0\\ 0 & 0 & \mathbb{R}\mathbf{n}_2'\cdot\mathbf{v}_{46} & \mathbb{R}\mathbf{n}_3'\cdot\mathbf{v}_{46}\\ 0 & 0 & \mathbb{R}\mathbf{n}_2'\cdot\mathbf{v}_{56} & \mathbb{R}\mathbf{n}_3'\cdot\mathbf{v}_{56}\end{bmatrix}, \quad \boldsymbol{\varepsilon} = \begin{bmatrix}\varepsilon_1\\ \varepsilon_2\\ \varepsilon_3\\ \varepsilon_4\end{bmatrix}$$

4.3 Truss delay error

The mapping of the single gauge error to delay follows the form:

$$\delta d(u,v) = \mathbf{g}_{NCV}(u,v)\boldsymbol{\varepsilon} \qquad (21)$$

$$\mathbf{g}_{NCV}(u,v) = \left[\mathbf{s}(u,v)\right]^T\mathbf{M}_{NCV}\frac{d\mathbf{L}(u,v)}{d\boldsymbol{\varepsilon}^T}$$

where the NCV mapping matrix is simply the first 2 and the last 2 columns of the full mapping matrix:

$$\mathbf{M}_{NCV} = \begin{bmatrix}-1.1652 & 0.5000 & -0.5000 & 1.1652\\ 0.1127 & 0.1470 & 0.1470 & 0.1127\\ 0.4237 & 0.5000 & -0.5000 & -0.4237\end{bmatrix} \qquad (22)$$

4.4 Zernike component matrix

One can define a Zernike component matrix for NCVE:

$$\boldsymbol{\gamma}_{NCV} = \frac{\varepsilon_{NCV}}{\sqrt{\pi}}\iint\limits_{x^2+y^2\le 1}\mathbf{Z}^{*T}(x,y)\left(\mathbf{g}_{NCV}(u,v)-\mathbf{g}_{NCV}(0,0)\right)dxdy \qquad (23)$$

$x = \dfrac{u}{R_{\max}}, \quad y = \dfrac{v}{R_{\max}}$, – integration is over FOR

$\mathbf{Z}(x,y) = \left[\mathcal{Z}_1 \quad \mathcal{Z}_2 \quad \ldots \quad \mathcal{Z}_{10}\right]$, $\mathcal{Z}_i$ – ith order Zernike Polynomial

$\varepsilon_{NCV} = \sqrt{\varepsilon_1^2+\varepsilon_2^2+\varepsilon_3^2+\varepsilon_4^2}$, - amplitude of the composite offset vector

5. DISCUSSION AND CONCLUSION

The advantage of the Zernike component matrix of the delay error corresponding to a particular type of error is that it can be conveniently combined with other model's corresponding Zernike component matrix to yield the full error metric matrix. Other effects that have been treated or estimated include corner cube surface index errors, race-track beam location errors, corner cube orientation errors. The interested reader is referred to Ref. 8 for relevant details. Future development of SIM external metrology system requirements will necessitate more careful assessment of errors based on given statistical distributions of error parameters.

ACKNOWLEDGEMENT

This work was performed at Jet Propulsion Laboratory, California Institute of Technology, under contract with the National Aeronautics and Space Administration.

REFERENCES

1. R. Danner and S. Unwin, eds., *SIM Interferometer Mission: Taking the Measure of the Universe*, NASA document JPL 400-811, 1999; also see http://sim.jpl.nasa.gov
2. J. Marr-IV et al., Space Interferometry mission (SIM): overview and current status," in *Interferometry in Space, Proc. SPIE* **4852**, 1-15 (2003).
3. L. Ames, S. D. Barrett, S. Calhoun, T. Kvamme, J. Mason, J. Oseas, M. Pryor, D. Schaecter, and D. Stubbs, Space Interferometry mission starlight and metrology subsystem, in *Interferometry in Space, Proc. SPIE* **4852**, 289-301 (2003).
4. M. H. Milman and S. G. Turyshev, Observational model for microarcsecond astrometry with the Space Interferometry Mission, *Opt. Eng.* 42(7), 1873-1883, 2003
5. J. Yu, Description of SIM Astrometric Error Budget, JPL Space Interferometry Mission Internal Library, Aug 20, 2002
6. B. Nemati, G. M. Kuan, Model validation of SIM external metrology at the sub-nanometer level, *Proc. SPIE Conference on Astronomical Telescopes and Instrumentation, Vol. 5491*, Glasgow, Scotland, June 2004 (in press).
7. Milman, M. H. and L. D. Zhang, Error modeling of multi-baseline optical truss, part I: ???, 5528A-??, this proceeding.
8. L. D. Zhang, M. Milman, L. Sievers, R. Korechoff, K. Aaron, L19 External Metrology Truss Field Dependent Error Model – Part I: Corner Cube Dihedral and Surface Index Error, JPL Space Interferometry Mission Internal Library, 05-18-2004